

Non-reciprocal interactions preserve the universality class of Potts model

Soumya K. Saha and P. K. Mohanty*

Department of Physical Sciences, Indian Institute of Science Education and Research Kolkata, Mohanpur, 741246 India.

(Dated: December 30, 2024)

We study the q -state Potts model on a square lattice with directed nearest-neighbor spin-spin interactions that are inherently non-reciprocal. Both equilibrium and non-equilibrium dynamics are investigated. Analytically, we demonstrate that non-reciprocal interactions do not alter the critical exponents of the model under equilibrium dynamics. In contrast, numerical simulations with selfish non-equilibrium dynamics reveal distinctive behavior. For $q = 2$ (non-reciprocal non-equilibrium Ising model), the critical exponents remain consistent with those of the equilibrium Ising universality class. However, for $q = 3$ and $q = 4$, the critical exponents vary continuously. Remarkably, a super-universal scaling function—Binder cumulant as a function of ξ_2/ξ_0 , where ξ_2 is the second moment correlation length and ξ_0 its maximum value—remains identical to that of the equilibrium $q = 3, 4$ Potts models. These findings indicate that non-reciprocal Potts models belong to the superuniversality class of their respective equilibrium counterparts.

The study of non-reciprocal interactions, where the influence of one component on another is asymmetric, has emerged as a frontier in statistical physics [1] due to their widespread occurrence across diverse systems, including active matter [2, 3], condensed matter [4–7], biological systems [8–10], and social systems [11]. Unlike conventional reciprocal interactions, non-reciprocal systems exhibit a range of novel phenomena, such as self-assembly [12], topological phases [13, 14], hyperuniform states [15], non-reciprocal synchronization [16], time-crystalline order [17], self-organization [18], and unconventional phase transitions [19–22].

In stochastic systems, non-reciprocal interactions drive complex dynamics. For instance, asymmetric neural networks studied by Sompolinsky and Kanter [23] exhibit altered temporal association dynamics. Similarly, non-reciprocal interactions are observed in colloidal systems with tunable anisotropy [12] and multicellular assemblies with asymmetric cell-cell communication [10]. Such interactions are also evident in catalytically driven particles [24] and soft matter systems [20].

Although non-reciprocal interactions appear to violate Newton’s third law of equal and opposite reaction [25], they have been experimentally demonstrated in systems such as micro-particles in anisotropic plasmas [26], motile particles in elastic media [27], programmable robots [19], optically levitated nanoparticles [28], micro-scale oil droplets in surfactant solutions [29], and ions interacting in plant cells [30]. Often, these interactions emerge as effective forces driven by collective activity, such as the persistent or chiral motion of active particles [2, 22] or molecular crowding in chemical systems. Recent studies even suggest that confined water can induce directed non-reciprocal interactions [31].

Despite extensive research in active matter systems [2], the implications of non-reciprocal interactions for equilibrium and non-equilibrium critical behavior remain poorly understood. In a recent study, Chen et al. [15] demonstrated emergent chirality and hyperuniformity in active

mixtures mediated by non-reciprocal interactions. Similarly, collective flocking dynamics have been observed in active fluids with non-reciprocal orientational interactions [22]. Non-reciprocal interactions can enhance heterogeneity [32], stabilize dynamical phases [33], and facilitate particle escape from kinetic traps [34].

To elucidate the nature of phase transitions, such as phase separation, crowding, flocking, or condensation in the presence of non-reciprocal interactions, several models have been proposed. The non-reciprocal Cahn-Hilliard model [21] provides a framework for understanding pattern formation in non-equilibrium systems. Time-delayed interactions, as studied by Durve et al. [35], further highlight their significance in active particle condensation. Additionally, non-reciprocal extensions of Ising [36, 37], XY [14], and Heisenberg [38] spin models have revealed modifications to phase behavior and scaling exponents.

In this Letter, we analyze the equilibrium and non-equilibrium dynamics of q -state Potts models with directed, non-reciprocal nearest-neighbor interactions on a square lattice. Our analytical results demonstrate that non-reciprocal interactions preserve critical exponents in equilibrium, maintaining universality class invariance. Numerical simulations with selfish non-equilibrium dynamics show that for $q = 2$ (Ising-spins), the critical exponents align with those of the equilibrium Ising model. For $q = 3$ and $q = 4$, continuously varying critical exponents are observed. However, the Binder cumulant reveals that it is super-universal scaling function of ξ_2/ξ_0 , which matches the equilibrium Potts model. These findings suggest the existence of a superuniversality class [39–43] bridging the critical behaviour of non-reciprocal Potts model with equilibrium and non-equilibrium dynamics.

The model: The model is defined on a periodic square lattice \mathcal{L} with sites labeled by $\mathbf{i} \equiv (x, y)$ with $x, y = 1, 2, \dots, L$. The neighbours of a site \mathbf{i} is denoted by $\mathbf{i} + \mathbf{e}_k$ where the unit vector $\mathbf{e}_k \equiv (\cos(\frac{\pi}{2}k), \sin(\frac{\pi}{2}k))$, with $k = 0, 1, 2, 3$. Each site \mathbf{i} is occupied by a spin $s_{\mathbf{i}}$

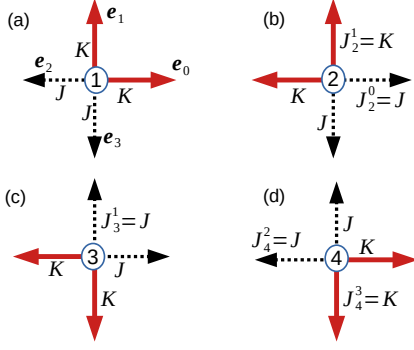


FIG. 1. (Color online) Four interaction configurations. (a) $s_i = 1$: interaction strength is K in right and up direction (thick line) and J in left and down direction (dashed line). (b),(c),(d) corresponds to $s_i = 2, 3, 4$. In general $s_i = s$ interact with its k -th neighbour (at $\mathbf{i} + \mathbf{e}_k$) with strength J_s^k given by Eq. (2). For the q -state Potts model we consider only first q interaction configurations.

which can be in one of q states, i.e., $s_i = 1, 2, \dots, q$. A spin s_i interacts with its k -th neighbors with interaction strength $J_{s_i}^k$ that depends explicitly on both the spin-value s_i and the direction of the neighbour k . (see Fig. 1 and descriptions there). Energy of any configuration $\{s_i\}$ is given by

$$E(\{s_i\}) = - \sum_{\mathbf{i} \in \mathcal{L}} \sum_{k=0}^3 J_{s_i}^k (2\delta_{s_i, s_i + \mathbf{e}_k} - 1). \quad (1)$$

Note that, $J_s^k > 0$ represents ferromagnetic interaction among spins, as energy of the system is lowered by making neighbouring spins parallel (same). Further, we specify the directional interaction as follows.

$$J_s^k = K(\delta_{s,k} + \delta_{s,k+1}) + J(\delta_{s,k-1} + \delta_{s,k-2}). \quad (2)$$

For example, when $s_i = 1$ the interaction occurs along the direction \mathbf{e}_0 and \mathbf{e}_1 with strength K (thick lines in Fig. 1 (a)) and the same occurs with spins in other two directions with strength J (broken lines in Fig. 1(a)). The energy can be written as $E(\{s_i\}) = E_x(\{s_i\}) + E_y(\{s_i\})$ where E_x and E_y are the contributions from bonds oriented in x (horizontal) and y (vertical) directions.

$$\begin{aligned} E_x(\{s_i\}) &= - \sum_{\mathbf{i} \in \mathcal{L}} J_{s_i, s_i + \mathbf{e}_0}^x (2\delta_{s_i, s_i + \mathbf{e}_0} - 1) \\ E_y(\{s_i\}) &= - \sum_{\mathbf{i} \in \mathcal{L}} J_{s_i, s_i + \mathbf{e}_1}^y (2\delta_{s_i, s_i + \mathbf{e}_1} - 1). \end{aligned} \quad (3)$$

Note that the sum over the sites counts exactly one horizontal and one vertical bond with interaction strengths

$$J_{s, \bar{s}}^x = J_s^0 + J_{\bar{s}}^2; \quad J_{s, \bar{s}}^y = J_s^1 + J_{\bar{s}}^3 \quad (4)$$

respectively. The non-reciprocal nature of the interaction is clear from the fact that $J_{s, \bar{s}}^{x,y} \neq J_{\bar{s}, s}^{x,y}$, which is evident from Eq. (2).

First we use a dynamics that satisfy detailed balance, where a configuration $\{\dots, s_i, \dots\}$ changes $\{\dots, \tilde{s}_i, \dots\}$ with the Metropolis rate $r = \text{Min}(1, e^{-\Delta E})$ where $\Delta E = E(\{\dots, \tilde{s}_i, \dots\}) - E(\{\dots, s_i, \dots\})$. This dynamics takes the system to equilibrium; the partition function at temperature T ($\beta = \frac{1}{k_B T}$, k_B is Boltzmann constant) is

$$Q(\beta) = \sum_{\{s_i\}} \prod_{\mathbf{i}} \langle s_i | M_x | s_{i+\mathbf{e}_0} \rangle \prod_{\mathbf{i}} \langle s_i | M_y | s_{i+\mathbf{e}_1} \rangle. \quad (5)$$

Here $M_{x,y}$ are $q \times q$ matrix with elements,

$$\langle s | M_{x,y} | \tilde{s} \rangle = e^{\beta J_{s, \tilde{s}}^{x,y} (2\delta_{s, \tilde{s}} - 1)}. \quad (6)$$

It turns out that matrices M_x and M_y do not commute, but they are isospectral; their eigenvalues are,

$$\begin{aligned} \lambda_1 &= \lambda_2 = \dots = \lambda_{q-1} = 2 \sinh(\beta(J + K)); \\ \lambda_q &= q \cosh(\beta(J + K)) - (q - 2) \sinh(\beta(J + K)). \end{aligned} \quad (7)$$

It is easy to check that both M_x and M_y are isospectral to another $q \times q$ matrix M with elements $\langle s | M | \tilde{s} \rangle = e^{\beta \epsilon (2\delta_{s, \tilde{s}} - 1)}$, that appears in the partition function of the ordinary q -state Potts model on a two dimensional square lattice with $H = -\epsilon \sum_{\mathbf{i}} \sum_{k=0}^3 (2\delta_{s_i, s_i + \mathbf{e}_k} - 1)$.

$$Q_{\text{Potts}}(\beta) = \sum_{\{s_i\}} \prod_{\mathbf{i}} \langle s_i | M | s_{i+\mathbf{e}_0} \rangle \prod_{\mathbf{i}} \langle s_i | M | s_{i+\mathbf{e}_1} \rangle. \quad (8)$$

Thus, the partition function of the non-reciprocal q -state Potts model with equilibrium dynamics can be exactly mapped onto that of the conventional reciprocal Potts model when $\epsilon = K + J$.

The q -state Potts models belong to the \mathbb{Z}_q universality class with their critical points (for a square lattice) and critical exponents known exactly [44],

$$\begin{aligned} \epsilon_c &= \ln(1 + \sqrt{q})T; \quad \mu = \frac{2}{\pi} \cos^{-1} \left(\frac{\sqrt{q}}{2} \right); \\ \nu &= \frac{2 - \mu}{3 - 3\mu}; \quad \beta = \frac{1}{12}(1 + \mu); \quad \gamma = \frac{7 - 4\mu + \mu^2}{6 - 6\mu}. \end{aligned} \quad (9)$$

We expect the phase transition in the non-reciprocal q -state Potts model to occur at $T = 1$, when interaction strength K crosses a threshold

$$K_c = -J + \ln(1 + \sqrt{q}). \quad (10)$$

with critical exponents for different q given by Eq. (9). We verify this from Monte Carlo simulations. We consider the usual order parameter of the Potts model: if number of sites having $s_i = k$ is N_k we have $L^2 = \sum_{k=1}^q N_k$. If the largest among the $\{N_k\}$ is N_{max} , the order parameter ϕ , the susceptibility χ , and the Binder cumulant U_4 are given by

$$\phi = \langle \mu \rangle; \quad \chi = \langle \mu^2 \rangle - \langle \mu \rangle^2; \quad U_4 = 1 - \frac{\langle \mu^4 \rangle}{3\langle \mu^2 \rangle^2};$$

$$\text{where } \mu = \frac{1}{q-1} \left(q \frac{N_{max}}{L^2} - 1 \right). \quad (11)$$

From Monte Carlo simulations we obtain μ and its moments to construct U_4, ϕ, χ . In the inset of Fig. 3 (a) and (b), we have shown the heat-map of the order parameter ϕ in the K - J plane for $q = 3, 4$, respectively. In each case, the color gradients naturally exhibit a straight line that separates the high ϕ -values from the low one. For some of the J values, we also obtain K_c accurately (shown as symbols) from the crossing point of the Binder cumulants U_4 ; they match with Eq. (10) and fall on the linear boundary of the order-disorder phase. The critical exponents all along this critical line are expected to be identical to those of the q -state Potts model, given in Eq. (9) [44].

We obtain the critical exponents $\beta, \gamma, \frac{\beta}{\nu}$ from finite size scaling [45] for different critical points (see Supplemental Material [46]). One can obtain it directly from simulating large system using the relations: $\phi \sim \epsilon^\beta, \chi \sim \epsilon^{-\gamma}$ where $\epsilon = K - K_c$, and $\phi \sim L^{\frac{\beta}{\nu}}$ at the critical point $\epsilon = 0$. For $T = 1, J = 0.2$, log-scale plot of ϕ and χ , obtained from simulations $L = 256$ for different ϵ are shown in Fig. 2 (a),(b); straight lines having slopes β and γ , taken from Eq. (9) for different q -values, are drawn along the data (symbols) for comparison. A good match suggests that the non-reciprocal interaction does not change the universality of the system when the dynamics follows detailed balance.

We now focus on the non-equilibrium dynamics, commonly referred to as the *selfish dynamics* [47]. In this dynamics, the spins at any site can change their values without affecting the energy of the neighboring spins. Let us rewrite the energy function in Eq. (1) as $E(\{s_i\}) = \sum_{i \in \mathcal{L}} E_i(s_i)$ where

$$E_i(s_i) = - \sum_{k=0}^3 J_{s_i}^k \left(2\delta_{s_i, s_i + e_k} - 1 \right). \quad (12)$$

In the selfish dynamics, a spin s_i at \mathbf{i} changes to a randomly chosen value $\tilde{s}_i \neq s_i$ with rate,

$$r = \text{Min}(1, e^{-\Delta E_i}) \text{ with } \Delta E_i = E_i(\tilde{s}_i) - E_i(s_i). \quad (13)$$

The term ΔE_i does not include the change of energy felt at neighboring sites when $s_i \rightarrow \tilde{s}_i$, justifying the name - selfish dynamics. This dynamics does not satisfy detailed balance condition wrt energy function (1) and it evolves the system to a non-equilibrium steady state (NESS). In NESS, the system exhibits a non-equilibrium phase transition from a disordered to a ordered state characterized by the order parameter ϕ , susceptibility χ and Binder cumulant U_4 defined in Eq. (11). For a fixed value of J , the crossing point of U_4 vs. K curve for different L gives us the critical value K_c and log-scale plot of ϕ, χ as a function of $\epsilon = K - K_c$ at $L = 256$ gives us the estimate of critical exponents β, γ . In addition, log-scale plot ϕ vs

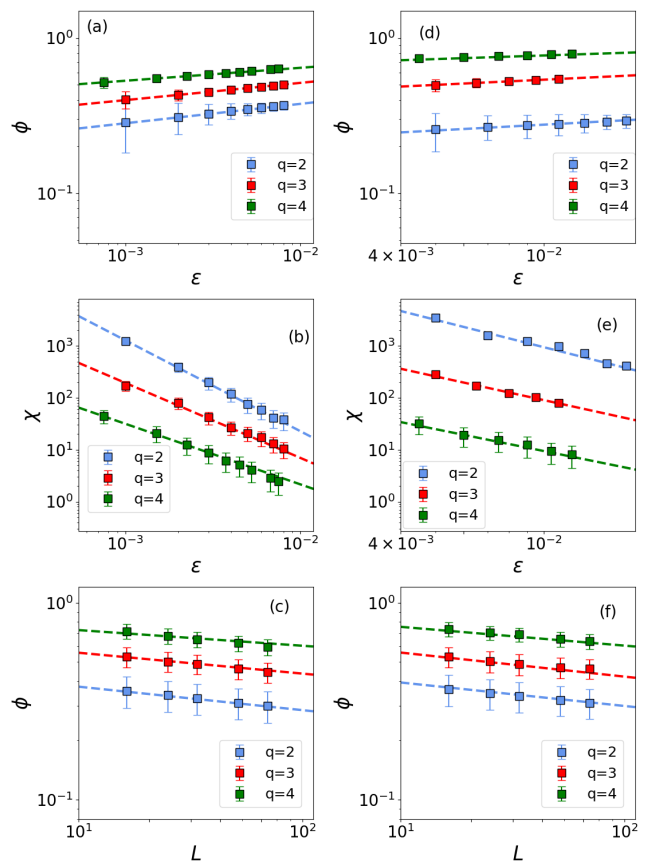


FIG. 2. (Color online) (a),(b),(c) Estimate of critical exponents $\beta, \gamma, \beta/\nu$ for non-reciprocal Potts model with equilibrium dynamics, at $J = 0.2$. (a), (b) shows log-scale plot of ϕ vs $\epsilon = K - K_c$ and χ vs ϵ for $L = 256$. (c) ϕ vs L at $K = K_c = 0.2407(q = 2), 0.3025(q = 3)$ and $0.3496(q = 4)$. Straight lines of slope $\beta, \gamma, \beta/\nu$ of $\mathbb{Z}_2, \mathbb{Z}_3$ and \mathbb{Z}_4 universality class (given in Eq. (9)) are drawn along the data for comparison. (d),(e),(f): The same for non-equilibrium dynamics with $J = 0.2, 0.4, 0.5$ respectively for $q = 2, 3, 4$, resulting in $K_c = 0.762, 0.614, 0.6065$. Slope of the best fit lines provide the estimate of $\beta, \nu, \beta/\nu$ (listed in table I for $q = 3, 4$, and for $q = 2$, we get Ising exponents $\beta = \frac{1}{8} = \beta/\nu$ and $\gamma = 7/4$). Data are averaged over 10^7 samples.

L at $K = K_c$ provides $\frac{\beta}{\nu}$. These curves are shown in Fig. 2 (d),(e) and (f); three different plots in each figure correspond to $q = 2, 3, 4$ and for $J = 0.2, 0.4, 0.5$ respectively. For $q = 2$, the estimate of critical exponents match with that of the equilibrium Ising model, whereas for $q = 3, 4$ they differ from respective exponents of equilibrium Potts model with $q = 3, 4$.

This led us to investigate the critical behavior all along the critical line shown in Fig. 3 (a),(b) respectively for $q = 3, 4$; there, the heat-map of order parameter ϕ in K - J plane appears in two different colors about the critical line. The resulting critical exponents, obtained from finite size scaling (described in Supplemental Material [46]) are listed in Table I. Clearly, the critical exponents

$q = 3$					$q = 4$				
J	K_c	β	γ	β/ν	J	K_c	β	γ	β/ν
0.300	0.738	0.160	1.586	0.168	0.500	0.606	0.069	1.40	0.090
0.400	0.614	0.111	1.517	0.128	0.525	0.576	0.080	1.44	0.100
0.503	0.503	0.111	1.444	0.133	0.549	0.549	0.083	1.17	0.125
0.614	0.400	0.111	1.517	0.128	0.576	0.525	0.080	1.44	0.100
0.738	0.300	0.160	1.586	0.168	0.606	0.500	0.069	1.40	0.090

TABLE I. Table of critical exponents for selfish dynamics.

of non-equilibrium non-reciprocal Potts model vary continuously when $q = 3$ or 4. Note that when $J = K$, the selfish dynamics is identical to that of the Potts model with equilibrium dynamics and thus, the critical exponents here (3rd row in Table I) are given by (9). Continuously varying exponents often emerge due to the presence of marginal operators. Recent studies [39–43] demonstrate that in such cases, the critical behavior forms a superuniversality class associated with the parent fixed point. Specifically, the superuniversal scaling function $U_4 = \mathcal{G}(\xi_2/\xi_0)$ remains invariant along the entire critical line. Here, ξ_0 represents the maximum value of the correlation length (finite for any finite L), while ξ_2 is the second-moment correlation length, defined as

$$(\xi_2)^2 = \frac{\int_0^\infty r^2 C(r) dr}{\int_0^\infty C(r) dr}, \quad \text{where } C(r) = \langle S_i \cdot S_{i+r} \rangle - \phi^2.$$

The spin variables S_i are constructed from the Potts state $s_i = k$ (with $1 \leq k \leq q$), corresponding to a unit vector representation: $S_i = (\cos \frac{2\pi k}{q}, \sin \frac{2\pi k}{q})$. Notably, the average magnitude of the total spin $\mathbf{S} = \frac{1}{L^2} \sum_i S_i$ in the steady state is given by $\langle \sqrt{\mathbf{S} \cdot \mathbf{S}} \rangle = \phi$.

To confirm the superuniversality scenario, we compute ξ_2 and ξ_0 from Monte Carlo simulations for various K values while keeping J and L fixed. The procedure is repeated for different J, L values. Using this data, we construct parametric plots of ξ_2/ξ_0 as a function of U_4 in Fig. 3(c) for $q = 3$ and in Fig. 3(d) for $q = 4$. These plots closely match the reference curve (dashed line) obtained from the standard $q = 3$ and $q = 4$ equilibrium Potts models with reciprocal interactions.

A few clarifications are in order. For $q = 2$, we have assigned the spin configurations (a) and (b) in Fig. 1 to $s_i = 1, 2$, respectively. Alternative configurations are equally valid. For instance, one could assign (a) and (c) to $s_i = 1, 2$; under this assignment, the model resembles the vision-cone interactions of Ising spins described in [48]. In fact, it is straightforward to show that for any of the six (four) possible interaction assignments, the isospectrality argument for equilibrium dynamics remains valid for both $q = 2$ and $q = 3$ cases. This robustness against interaction assignments reaffirms that non-reciprocity does not alter the universality class of

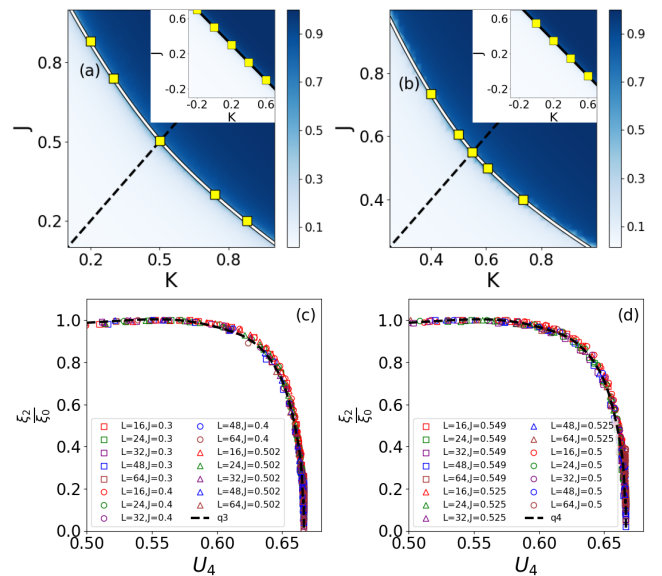


FIG. 3. (Color online)(a),(b) Density plots of the order parameter ϕ in the K - J plane for the non-reciprocal Potts model with selfish non-equilibrium dynamics for $q = 3, 4$. The critical line separates the ordered phase (darker colors) from the disordered phase, with symbols marking the critical points at which the critical behavior is analyzed. The resulting critical exponents are listed in Table I. The insets show the same data for equilibrium dynamics, where the linear critical line agrees with the prediction from Eq. (10). (c),(d) Superuniversal scaling function: ξ_2/ξ_0 vs. the Binder cumulant U_4 for $q = 3, 4$ respectively. The data (symbols), obtained by varying K for different values of J and L , collapse onto a single curve, which matches the equilibrium $q = 3, 4$ Potts model.

systems with discrete symmetry.

Additionally, interchanging J and K corresponds merely to a different spin assignment, leaving the critical line symmetric. In other words, if (J, K) is a critical point, so is (K, J) . This symmetry is evident from Eq. (10) for equilibrium dynamics and is also reflected in Fig. 3 for non-equilibrium dynamics.

In summary, we investigated the effects of non-reciprocal interactions in two-dimensional systems with discrete symmetry, exemplified by the q -state Potts model. In equilibrium, the model exhibits continuous phase transitions for $q = 2, 3, 4$, breaking discrete symmetries $\mathbb{Z}_2, \mathbb{Z}_3, \mathbb{Z}_4$, respectively, while for $q > 4$, the transitions become discontinuous. The universality classes of the continuous transitions are characterized by the critical exponents given in Eq. (9).

When non-reciprocal interactions are introduced, the $q = 2$ model (Ising system) undergoes continuous phase transitions belonging to the Ising universality class, irrespective of whether the dynamics satisfy detailed balance (equilibrium) or violate it (selfish dynamics). For $q = 3$ and $q = 4$, the critical exponents in equilibrium align with the \mathbb{Z}_3 and \mathbb{Z}_4 universality classes, re-

spectively. However, under selfish dynamics, the system exhibits non-equilibrium phase transitions with continuously varying critical exponents. Despite this variation, a superuniversality class emerges, characterized by invariant super-universal scaling functions along the critical line, even when critical exponents vary.

Overall, our findings reveal that in two dimensions, non-reciprocity does not alter the universality class of phase transitions breaking discrete symmetries. The scenario for systems with continuous symmetries, however, could be fundamentally different. In equilibrium, continuous symmetries cannot be broken to produce true long-range order, yet such systems exhibit exotic phases in two dimensions and exceptional phase transitions in the presence of non-reciprocal interactions [19].

* pkmohanty@iiserkol.ac.in

- [1] M. J. Bowick, N. Fakhri, M. C. Marchetti, and S. Ramaswamy, Symmetry, thermodynamics, and topology in active matter, *Phys. Rev. X* **12**, 010501 (2022).
- [2] A. Dinelli, J. O’Byrne, A. Curatolo, Y. Zhao, P. Sollich, and J. Tailleur, Non-reciprocity across scales in active mixtures, *Nat. Comm.* **14**, 7035 (2023).
- [3] C. Bechinger, R. D. Leonardo, H. Löwen, C. Reichhardt, G. Volpe, and G. Volpe, Active particles in complex and crowded environments, *Rev. Mod. Phys.* **88**, 045006 (2016).
- [4] T. Liu, J.-Y. Ou, K. F. MacDonald, and N. I. Zheludev, Photonic metamaterial analogue of a continuous time crystal, *Nat. Phys.* **19**, 986 (2023).
- [5] M. Reisenbauer, H. Rudolph, L. Egved, K. Hornberger, A. V. Zasedatelev, M. Abuzarli, B. A. Stickler, and U. DeliĆ, Non-hermitian dynamics and non-reciprocity of optically coupled nanoparticles, *Nat. Phys.* **10**, 1629 (2024).
- [6] V. Raskatla, T. Liu, J. Li, K. F. MacDonald, and N. I. Zheludev, Continuous space-time crystal state driven by nonreciprocal optical forces, *Phys. Rev. Lett.* **133**, 136202 (2024).
- [7] C. A. Downing and Z. D., Non-reciprocal population dynamics in a quantum trimer, *Proc. R. Soc. A* **477**, 20210507 (2021).
- [8] S. H. L. Klapp, Non-reciprocal interaction for living matter, *Nat. Nanotech.* **18**, 8 (2023).
- [9] D. J. Hickey, R. Golestanian, and A. Vilfan, Nonreciprocal interactions give rise to fast cilium synchronization in finite systems, *Proc. Nat. Acad. Sc.* **120**, e2307279120 (2023).
- [10] B. Bhattacharjee, M. Hayakawa, and T. Shibata, Structure formation induced by non-reciprocal cell-cell interactions in a multicellular system, *Soft Matter* 10.1039/D3SM01752D (2023).
- [11] S. Xie, R. Ye, X. Li, Z. Huang, S. Cao, W. Lv, H. He, P. Zhang, Z. Fang, J. Zhang, and W. Song, Nonreciprocal interactions in crowd dynamics: Investigating the impact of moving threats on pedestrian speed preferences, *Transp. Res. C* **162**, 104586 (2024).
- [12] S. F. Navas and S. H. L. Klapp, Impact of non-reciprocal interactions on colloidal self-assembly with tunable anisotropy, *J. Chem. Phys.* 10.1063/5.0214730 (2023).
- [13] J. D. Töpfer and R. Fleury, Non-reciprocal topological phases in coupled oscillator networks, *Phys. Rev. X* **12**, 011045 (2022).
- [14] Y. Rouzairé, D. Levis, and I. Pagonabarraga, Non-reciprocal interactions reshape topological defect annihilation, arXiv:2401.12637 10.48550/arXiv.2401.12637 (2024).
- [15] J. Chen, X. Lei, Y. Xiang, M. Duan, X. Peng, and H. P. Zhang, Emergent chirality and hyperuniformity in an active mixture with nonreciprocal interactions, *Phys. Rev. Lett.* **132**, 118301 (2024).
- [16] C. Ho, L. Jutras-Dubé, M. L. Zhao, G. Mönke, I. Z. Kiss, and A. A., Nonreciprocal synchronization in embryonic oscillator ensembles, *Proc. Nat. Acad. Sc.* **121**, e2401604121 (2024).
- [17] R. Hanai, Nonreciprocal frustration: Time crystalline order-by-disorder phenomenon and a spin-glass-like state, *Phys. Rev. X* **14**, 011029 (2024).
- [18] S. Osat and R. Golestanian, Non-reciprocal multifarious self-organization, *Nat. Nanotech.* **18**, 79 (2023).
- [19] M. Fruchart, R. Hanai, P. B. Littlewood, and V. Vitelli, Non-reciprocal phase transitions, *Nature* **592**, 363 (2021).
- [20] N. P. Kryuchkov, A. V. Ivlev, and S. O. Yurchenko, Dissipative phase transitions in systems with nonreciprocal effective interactions, *Soft Matter* **14**, 9720 (2018).
- [21] S. Saha, J. Agudo-Cañalejo, and R. Golestanian, Scalar active mixtures: The nonreciprocal cahn-hilliard model, *Phys. Rev. X* **10**, 041009 (2020).
- [22] M. Knežević, W. T., and S. H., Collective motion of active particles exhibiting non-reciprocal orientational interactions, *Scientific Reports* 10.1038/s41598-022-23597-9 (2022).
- [23] H. Sompolinsky and I. Kanter, Temporal association in asymmetric neural networks, *Phys. Rev. Lett.* **57**, 2861 (1986).
- [24] N. Mandal, A. Sen, and R. D. Astumian, A molecular origin of non-reciprocal interactions between interacting active catalysts, SSRN 10.1016/j.chempr.2023.11.017 (2024).
- [25] A. V. Ivlev, J. Bartnick, M. Heinen, C.-R. Du, V. Nosenko, and H. Löwen, Statistical mechanics where newton’s third law is broken, *Phys. Rev. X* **5**, 011035 (2015).
- [26] E. A. Lisin, O. F. Petrov, E. A. Sametov, O. S. Vaulina, K. B. Statsenko, M. M. Vasiliev, J. Carmona-Reyes, and T. W. Hyde, Experimental study of the nonreciprocal effective interactions between microparticles in an anisotropic plasma, *Sci. Rep.* **10**, 13653 (2020).
- [27] R. K. Gupta, R. Kant, H. Soni, A. K. Sood, and S. Ramaswamy, Active nonreciprocal attraction between motile particles in an elastic medium, *Phys. Rev. E* **105**, 064602 (2022).
- [28] J. Rieser, M. A. Ciampini, H. Rudolph, N. Kiesel, K. Hornberger, B. A. Stickler, M. Aspelmeyer, and U. DeliĆ, Tunable light-induced dipole-dipole interaction between optically levitated nanoparticles, *Science* **377**, 987 (2022).
- [29] C. H. Meredith, P. G. Moerman, J. Groenewold, Y.-J. Chiu, W. K. Kegel, A. van Blaaderen, and L. D. Zarzar, Predator–prey interactions between droplets driven by

- non-reciprocal oil exchange, *Nat. Chem.* **12**, 1136 (2020).
- [30] H. J. Kronzucker, M. W. Szczerba, L. M. Schulze, and D. T. Britto, Non-reciprocal interactions between k^+ and na^+ ions in barley, *J. Expt. Bot.* **59**, 2793 (2008).
- [31] F. Jiménez-Ángeles, K. J. Harmon, T. D. Nguyen, P. Fenter, and M. Olvera de la Cruz, Nonreciprocal interactions induced by water in confinement, *Phys. Rev. Res.* **2**, 043244 (2020).
- [32] T. Carletti and R. Muolo, Non-reciprocal interactions enhance heterogeneity, *Chaos, Soliton Fract.* **164**, 112638 (2022).
- [33] E. I. R. Chiacchio, A. Nunnenkamp, and M. Brunelli, Nonreciprocal dicke model, *Phys. Rev. Lett.* **131**, 113602 (2023).
- [34] S. Osat, J. Metson, M. Kardar, and R. Golestanian, Escaping kinetic traps using nonreciprocal interactions, *Phys. Rev. Lett.* **133**, 028301 (2024).
- [35] M. Durve, A. Saha, and A. Sayeed, Active particle condensation by non-reciprocal and time-delayed interactions, *Euro. Phys. J. E* **41**, 10.1140/epje/i2018-11653-4 (2018).
- [36] Y. Avni, M. Fruchart, D. Martin, D. Seara, and V. Vitelli, The non-reciprocal ising model, arXiv:2311.05471 10.48550/arXiv.2311.05471 (2023).
- [37] A. K. Rajeev and A. V. A. Kumar, Ising model with non-reciprocal interactions, arXiv:2403.06875 (2024).
- [38] N. Bhatt, S. Mukerjee, and S. Ramaswamy, Emergent hydrodynamics in a non-reciprocal classical isotropic magnet, arXiv:2312.16500 10.48550/arXiv.2312.16500 (2023).
- [39] G. Delfino and E. Tartaglia, On superuniversality in the q -state potts model with quenched disorder, *Journal of Statistical Mechanics: Theory and Experiment* **2017**, 123303 (2017).
- [40] C. Bonati, A. Pelissetto, and E. Vicari, Phase diagram, symmetry breaking, and critical behavior of three-dimensional lattice multiflavor scalar chromodynamics, *Phys. Rev. Lett.* **123**, 232002 (2019).
- [41] I. Mukherjee and P. K. Mohanty, Hidden superuniversality in systems with continuous variation of critical exponents, *Phys. Rev. B* **108**, 174417 (2023).
- [42] S. K. Saha, A. Banerjee, and P. K. Mohanty, Site-percolation transition of run-and-tumble particles, *Soft Matter* **20**, 9503 (2024).
- [43] A. Banerjee, P. Jana, and P. K. Mohanty, Geometric percolation of spins and spin-dipoles in ashkin-teller model (2024), arXiv:2411.11644.
- [44] R. J. Baxter, *Exactly Solved Models in Statistical Mechanics* (Academic Press, London, 1982).
- [45] H. E. Stanley, *Introduction to Phase Transition and Critical Phenomena* (Oxford University Press, New York, 1971).
- [46] *Supplemental Material* (Here we report on estimation of critical exponents for different points on the critical line.).
- [47] Y. Avni, M. Fruchart, D. Martin, D. Seara, and V. Vitelli, Dynamical phase transitions in the non-reciprocal ising model, arXiv:2409.07481 10.48550/arXiv.2409.07481 (2024).
- [48] A. Garcés and D. Levis, Phase transitions in single species ising models with non-reciprocal couplings, arXiv:2411.03544 (2024).

Supplementary Material for: Non-reciprocal interactions preserve the universality class of Potts model

Soumya K. Saha and P. K. Mohanty*

Department of Physical Sciences, Indian Institute of Science Education and Research Kolkata, Mohanpur, 741246 India.

(Dated: December 30, 2024)

In this Supplemental Material, we present a finite size scaling (FSS) analysis [1] to investigate the critical behavior of the non-equilibrium q -state Potts model. This includes both the equilibrium dynamics, which obey detailed balance, and the selfish (non-equilibrium) dynamics as defined in the main text.

CRITICAL BEHAVIOR

We numerically investigate the critical behavior of the non-reciprocal Potts model defined in the main text using Monte Carlo simulations. Two types of dynamics are employed. The first is an equilibrium dynamics that drives the system to an equilibrium state with a Boltzmann distribution with respect to a non-reciprocal energy function. We explicitly demonstrate that this equilibrium state can also be achieved from a Hamiltonian with reciprocal interactions between spins, where the non-reciprocal interaction parameters K and J uniquely map to the strengths of the reciprocal interactions. This indicates that the non-reciprocal interactions do not alter the critical behavior of the q -state Potts model. To verify this explicitly, we calculate the critical exponents through Monte Carlo simulations of the model.

For the q -state Potts model [2], each spin s_i can occupy one of q states, $s_i = 1, 2, \dots, q$. In a given configuration, let N_k denote the number of sites with $s_i = k$, and let N_{max} represent the largest among the N_k . The order parameter ϕ , susceptibility χ , and Binder cumulant U_4 of the system are defined as:

$$U_4 = 1 - \frac{\langle \mu^4 \rangle}{3\langle \mu^2 \rangle^2}; \quad \phi = \langle \mu \rangle; \quad \chi = \langle \mu^2 \rangle - \langle \mu \rangle^2; \quad \text{where } \mu = \frac{1}{q-1} \left(q \frac{N_{max}}{L^2} - 1 \right) \quad (1)$$

where L is the linear size of the system, and $\langle \dots \rangle$ denotes ensemble averaging. These quantities serve to characterize the phase transitions and critical behavior under both equilibrium and non-equilibrium dynamics. To obtain the static critical exponents ν, β, γ we employ the finite size scaling analysis [1],

$$U_4 = f_b(\epsilon L^{\frac{1}{\nu}}); \quad \phi = L^{-\frac{\beta}{\nu}} f_\phi(\epsilon L^{\frac{1}{\nu}}); \quad \chi = L^{\frac{\gamma}{\nu}} f_\chi(\epsilon L^{\frac{1}{\nu}}). \quad (2)$$

Our approach is as follows: For a fixed value of J , we calculate ϕ , χ , and U_4 as defined in Eq. (1). This process is repeated for various system sizes $L = 16, 24, 32, 48, 64$. From the crossing points of the Binder cumulants U_4 versus K for different L , we determine the critical value K_c . Using this, we compute $\epsilon = K - K_c$.

Next, we plot U_4 as a function of $\epsilon L^{1/\nu}$ for different L and adjust the fitting parameter $1/\nu$ to collapse the curves onto a single master curve. Once $1/\nu$ is determined, we proceed by separately plotting $\phi L^{\beta/\nu}$ and $\chi L^{\gamma/\nu}$ against $\epsilon L^{1/\nu}$. The fitting parameters in these cases are β/ν and γ/ν , respectively, which are adjusted to achieve the best data collapse. This method provides accurate estimates of $\frac{1}{\nu}$, $\frac{\beta}{\nu}$, and $\frac{\gamma}{\nu}$.

In all figures below, the inset of panel (a) shows U_4 versus $\epsilon = K - K_c$, with the curves crossing at $\epsilon = 0$ (i.e., $K = K_c$). The main panel (a) displays the collapse of U_4 as a function of $\epsilon L^{1/\nu}$, yielding an estimate of $\frac{1}{\nu}$. Similarly, panels (b) and (c) show the collapse of $\phi L^{\beta/\nu}$ and $\chi L^{\gamma/\nu}$ versus $\epsilon L^{1/\nu}$, respectively, allowing us to determine $\frac{\beta}{\nu}$ and $\frac{\gamma}{\nu}$. The insets of panels (b) and (c) show the raw-data, before collapse. An independent estimate these exponents gives us an opportunity to verify the hyperscaling relation $d\nu = 2\beta + \gamma$ [2].

The same methodology is applied to estimate the critical exponents for the selfish non-equilibrium spin dynamics.

* pkmohanty@iiserkol.ac.in

[1] *Introduction to Phase Transition and Critical Phenomena*, H. E. Stanley, Oxford University Press, New York (1971).

[2] *Exactly Solved Models in Statistical Mechanics*, J. Baxter, Academic Press, London (1982).

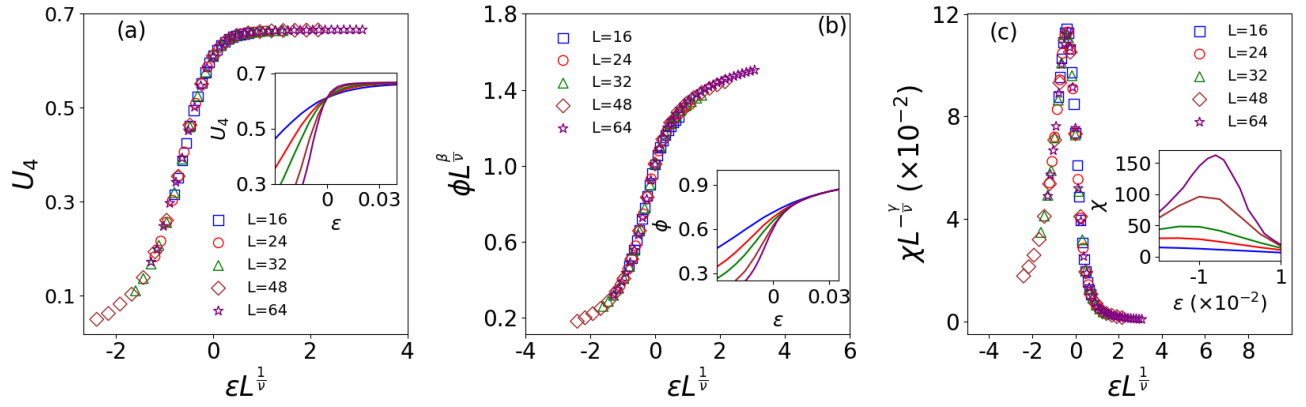


FIG. 1: From FSS, critical exponents obtained are (a) $\frac{1}{\nu} = 1$, (b) $\frac{\beta}{\nu} = 0.125$ and (c) $\frac{\gamma}{\nu} = 1.75$ for $q = 2$ equilibrium dynamics corresponding to the critical point $J = 0.2, K_c = 0.2407$

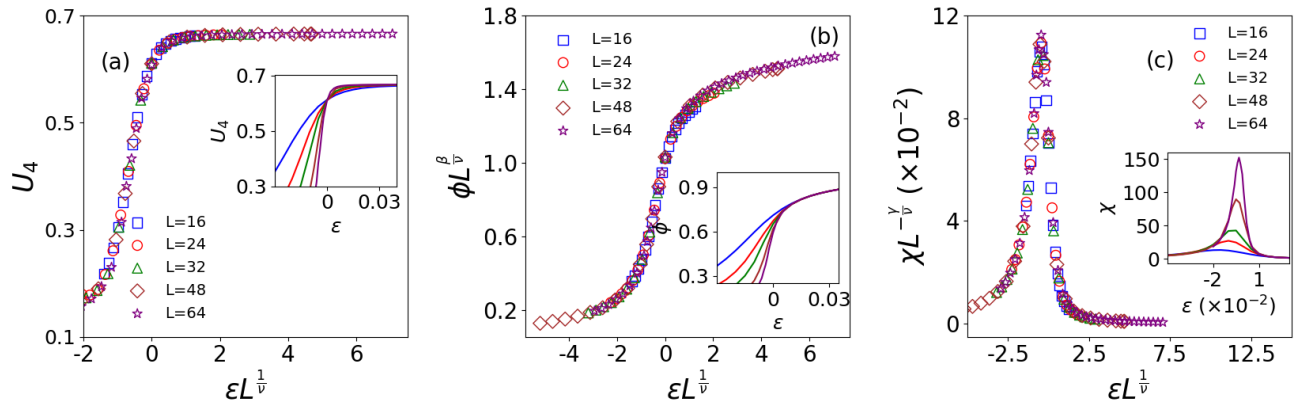


FIG. 2: From FSS, critical exponents obtained are (a) $\frac{1}{\nu} = 1.2$, (b) $\frac{\beta}{\nu} = 0.133$ and (c) $\frac{\gamma}{\nu} = 1.733$ for $q = 3$ equilibrium dynamics corresponding to the critical point $J = 0.2, K_c = 0.3025$.

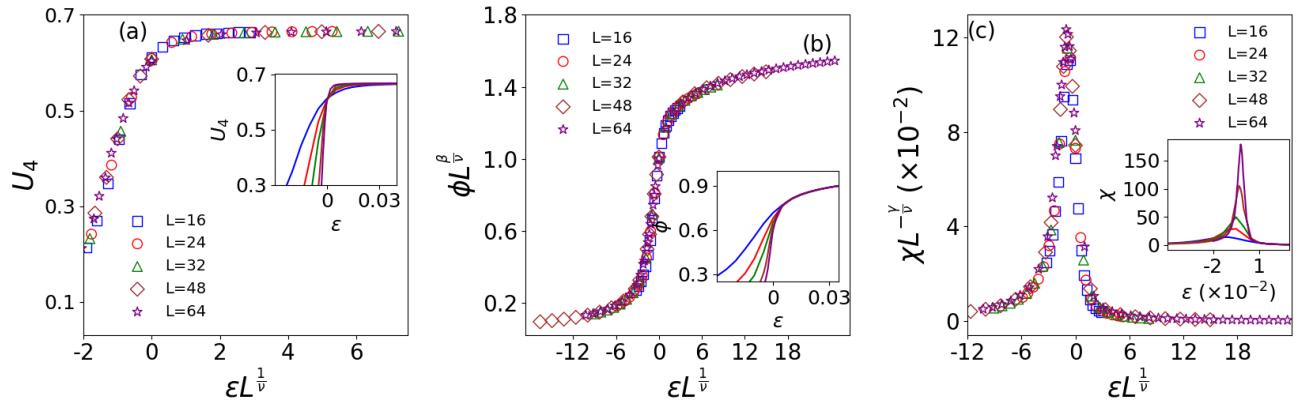


FIG. 3: From FSS, critical exponents obtained are (a) $\frac{1}{\nu} = 1.5$, (b) $\frac{\beta}{\nu} = 0.125$ and (c) $\frac{\gamma}{\nu} = 1.75$ for $q = 4$ equilibrium dynamics corresponding to the critical point $J = 0.2, K_c = 0.3493$

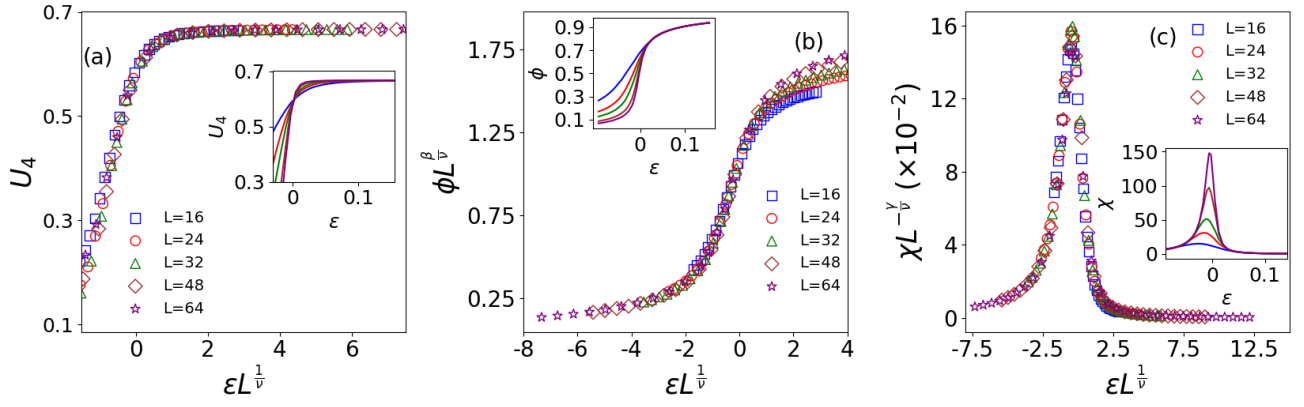


FIG. 4: From FSS, critical exponents obtained are (a) $\frac{1}{\nu} = 1.05$, (b) $\frac{\beta}{\nu} = 0.168$ and (c) $\frac{\gamma}{\nu} = 1.665$ for $q = 3$ selfish dynamics corresponding to the critical point $J = 0.3, K_c = 0.738$

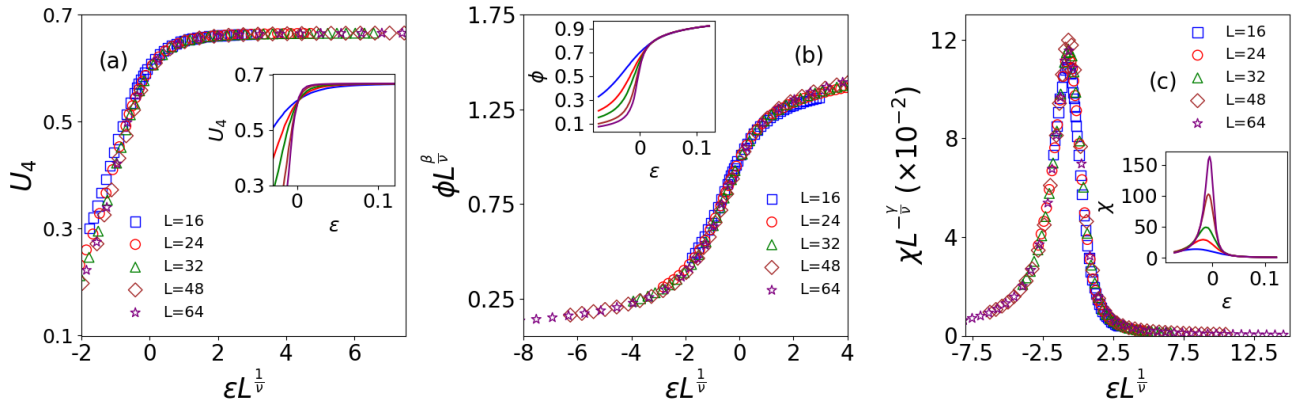


FIG. 5: From FSS, critical exponents obtained are (a) $\frac{1}{\nu} = 1.15$, (b) $\frac{\beta}{\nu} = 0.128$ and (c) $\frac{\gamma}{\nu} = 1.744$ for $q = 3$ selfish dynamics corresponding to the critical point $J = 0.4, K_c = 0.614$

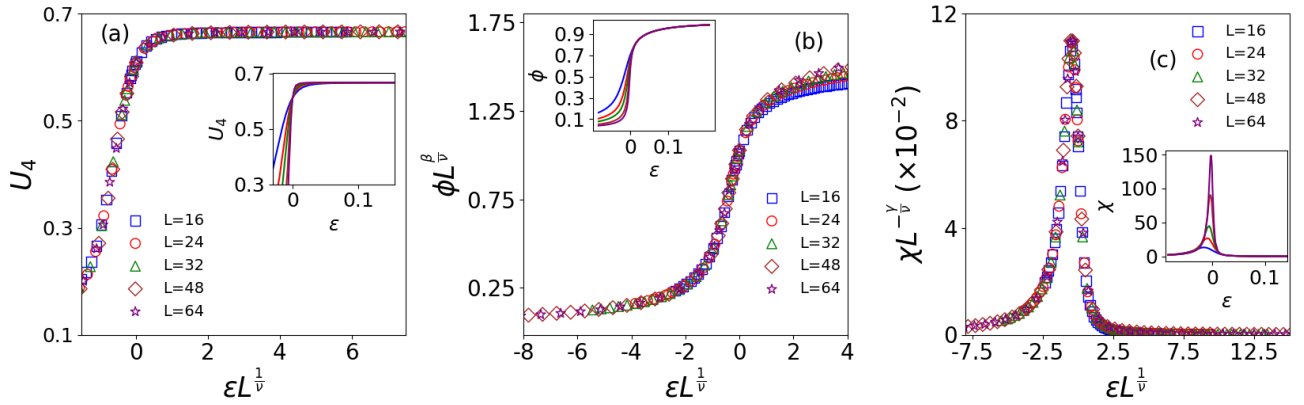


FIG. 6: From FSS, critical exponents obtained are (a) $\frac{1}{\nu} = 1.2$, (b) $\frac{\beta}{\nu} = 0.133$ and (c) $\frac{\gamma}{\nu} = 1.733$ for $q = 3$ selfish dynamics corresponding to the critical point $J = 0.5025, K_c = 0.5025$

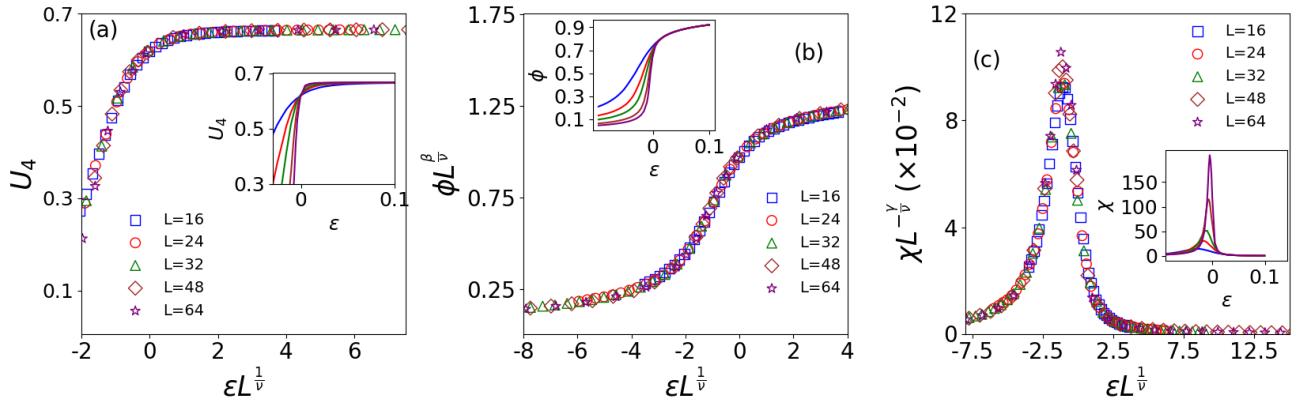


FIG. 7: From FSS, critical exponents obtained are (a) $\frac{1}{\nu} = 1.3$, (b) $\frac{\beta}{\nu} = 0.1$ and (c) $\frac{\gamma}{\nu} = 1.8$ for $q = 4$ selfish dynamics corresponding to the critical point $J = 0.5, K_c = 0.6065$

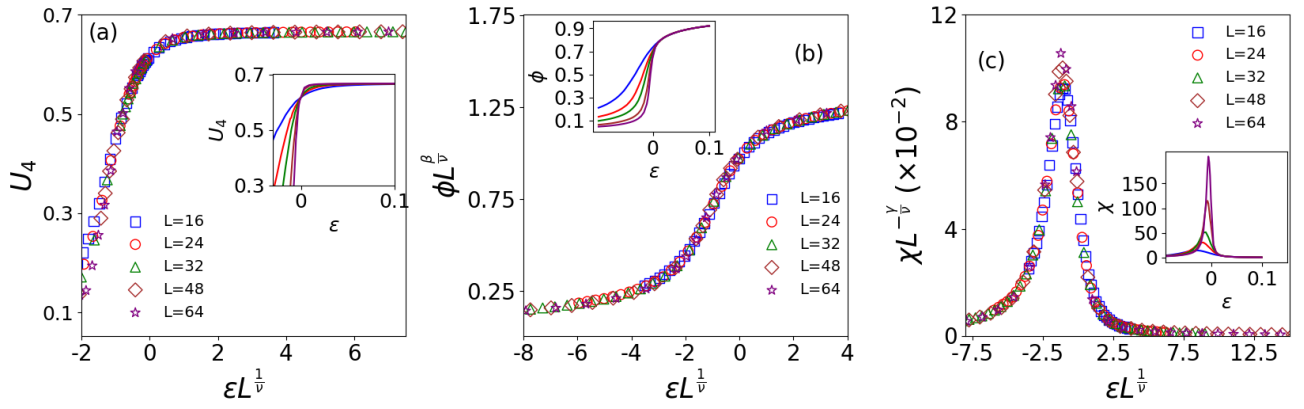


FIG. 8: From FSS, critical exponents obtained are (a) $\frac{1}{\nu} = 1.25$, (b) $\frac{\beta}{\nu} = 0.1$ and (c) $\frac{\gamma}{\nu} = 1.8$ for $q = 4$ selfish dynamics corresponding to the critical point $J = 0.525, K_c = 0.5765$

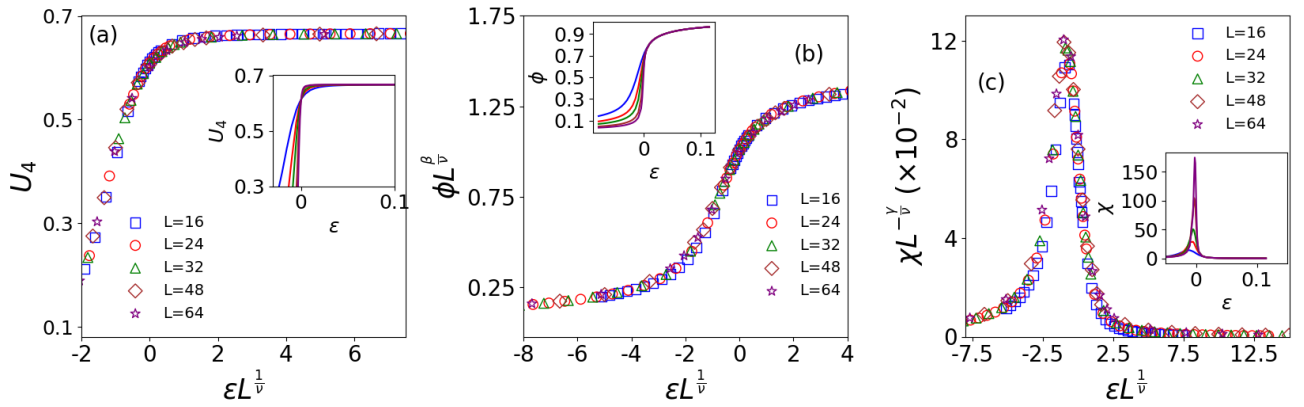


FIG. 9: From FSS, critical exponents obtained are (a) $\frac{1}{\nu} = 1.5$, (b) $\frac{\beta}{\nu} = 0.125$ and (c) $\frac{\gamma}{\nu} = 1.75$ for $q = 4$ selfish dynamics corresponding to the critical point $J = 0.5495, K_c = 0.5495$